International Journal of Engineering and Advanced Research Technology (IJEART)
ISSN: 2454-9290, Volume-4, Issue-1, January 2018

DEM Study on Flow Characteristics of Granular Material in a Heat Exchanger with Immersed Tubes

Daichang Guo, Bin Zheng, Haotian Liang, Yongqi Liu, Peng Sun

Abstract— **The heat exchanger with immersed tubes is one of the core equipment for recovering the waste heat of semi-coke. The particle flow in the heat exchanger is closely related to its heat exchange efficiency. In order to clarify the flow characteristics of semi-coke particles in the heat exchanger, a numerical calculation model of the heat exchanger was established by the discrete element method (DEM) in this paper. The process of particle flow in the heat exchanger was simulated by the model. The evolution of flow patterns, residence times and average velocity distributions of particles in the heat exchanger were analyzed. The results show that though the immersed tubes have a significant influence on the particle flow, the uniformity of the particle flow is good. There are major flow region of the center, major flow regions of the left and the right, flow around regions and boundary layers in the heat exchanger. The movement of particles in major flow region of the center is the fastest, in major flow region of the left or the right is the next, and in a flow around region or a boundary layer is the slowest.**

Index Terms— **Discrete Element Method, Flow characteristics, Heat exchanger, Immersed tubes, Semi-coke.**

I. Introduction

Heat exchangers for recovering waste heat are applied widely in many industries, e.g., for flue gas in chemical industry, slag in metallurgical industry, and coke in coal industry. One kind of heat exchanger with immersed tubes is proposed to recover the waste heat for semi-coke in this paper, as shown in Fig. 1. Although immersed tubes or tube bundle are helpful to increases the heat exchange area, and enhance the heat transfer ability by immersing into bulk material, there is a great influence of tube bundle on the particle flow in the heat exchanger. The impact of the particle flow in the heat exchanger on the heat transfer coefficient for particle-particle and particle-wall is significant [1]. Therefore, it is necessary to understand the behavior of the particle flow.

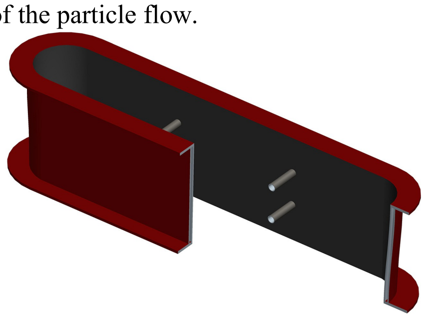

Fig. 1 Schematic illustration of heat exchanger with immersed tubes

A number of studies have been undertaken to investigate the behavior of the particle flow. Kondic et al. [2] discussed the flow of disk-like particles in the hopper using discrete element method. Yu et al. [3] studied the flow of mono-sized glass particles and analyzed the flow patterns and velocity distributions in a 3D conical hopper using the discrete element method. Many researches were focused on the discharge process of grains in a silo or hopper, such as the discharge of brown rice from a 3D conical silo [4], the discharge of maize grains from a small model silo [5]. Some studies have found that the placement of inserts has a significant influence on the flow behaviors [6]. Wu et al. [7] studied the flow characteristics of solid particles in a silo and analyzed the dependence of flow behaviors on the inserts used in a silo. Yang et al. [8] found that two kinds of inserts used in the silo can change the flow fields of the silo.

Most of the present studies focus on the particle flow in silos or hoppers, in which no insert or single insert is used. There are few reports on the particle flow in a flow channel with tube bundle, such as the heat exchanger with immersed tubes. Therefore, the discrete element simulation for the process of the particle flow in the heat exchanger was carried out in this paper. The evolution of flow patterns, residence times and average velocity distributions of particles in the heat exchanger are analyzed, which provide theoretical guidance for the design of the heat exchanger.

II. Model Description

A. Geometric model

The same size of the discrete element geometric model was set up according to the structure of the heat exchanger, as shown in Fig. 2. The dimensionless width of the heat exchanger is L=1. Therefore, the height is H=0.27, the horizontal distance between tubes is x=0.33, and the vertical distance between tubes is z=0.09. There is baffle at the bottom of the heat exchanger to control the movement of particles. At every beginning, particles are filled into the model uniformly until particles are almost full of storage area, as shown in Fig. 2. These particles are then allowed to settle under gravity to a stable condition. In the simulation, a tracer layer, which is laid at the inlet of the heat exchanger, is introduced to make it possible to observe and analyze the flow patterns during the process of the particle flow. When the simulation starts, the baffle moves downward at a fixed speed of 6×10^{-4} m/s. The particles move downward simultaneously controlled by baffle until the tracer layer flow out the heat exchanger completely.

The semi-coke particles are simplified into uniform spherical particles, because of its irregular shapes and different sizes. The physical properties of semi-coke particle

This study was supported by National Key R&D Program of China under Project No. 2017YFB0603504-2, and Shandong Provincial Natural Science Foundation, China (Grant Nos. ZR2017LEE019, ZR2014EL030).

and the wall used in the simulation are reported in Table 1.

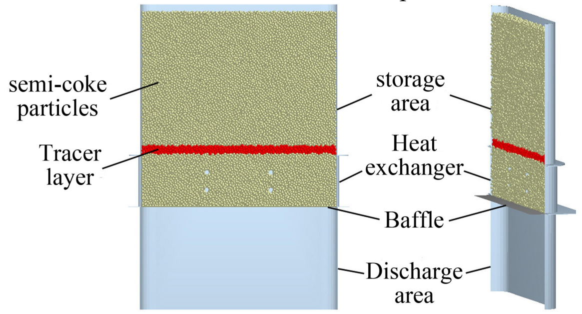

Fig. 2 Discrete element geometric model

Table 1 Physical properties and their values in the simulation

Type	Parameter	Value
Semi-coke particle	Density, ρ_p (Kg/m^3)	1000
	Poission's ratio	0.3
	Shear modulus, G_p (Pa)	1×10^8
	Diameter, d_p (mm)	40
Heat exchanger	Density, ρ_w (Kg/m^3)	7800
	Poission's ratio	0.3
	Shear modulus, G_p (Pa)	7×10^{10}
Particle-particle	Coefficient of static friction	0.6
	Coefficient of rolling friction	0.05
	Coefficient of restitution	0.5
Particle-wall	Coefficient of static friction	0.4
	Coefficient of rolling friction	0.05
	Coefficient of restitution	0.5

B. Mathematical model

In this work, the motions of individual particles are determined by the Newton's second law of motion which is defined by (1). The forces and torques due to gravity, deformation due to collisions, and rolling friction are considered for a particle i in contact with particle j as follows:

$$\begin{cases} m_i \dfrac{\partial \boldsymbol{v}_i}{\partial t} = \sum \boldsymbol{F} + m_i \boldsymbol{g} \\ I_i \dfrac{\partial \boldsymbol{\omega}_i}{\partial t} = \sum \boldsymbol{T} \end{cases} \tag{1}$$

where m_i, $\boldsymbol{g}$, I_i, $\boldsymbol{v}_i$ and $\boldsymbol{\omega}_i$ are the mass, acceleration of gravity, moment of inertia, translational velocity and rotational velocity of particle i, respectively. $\boldsymbol{F}$ and $\boldsymbol{T}$ are total contact force and total torque of particle i.

The discrete element simulation carried out in this work uses the Hertz–Mindlin contact model. The contact force can be broken down into normal and tangential contact forces which are defined by (2), (3), (4) and (5). The normal elastic force $\boldsymbol{F}^{\mathrm{n}}_{\mathrm{c},ij}$, normal damping force $\boldsymbol{F}^{\mathrm{n}}_{\mathrm{d},ij}$, tangential elastic force $\boldsymbol{F}^{\mathrm{t}}_{\mathrm{c},ij}$ and tangential damping force $\boldsymbol{F}^{\mathrm{t}}_{\mathrm{d},ij}$ are respectively given by:

$$\boldsymbol{F}^{\mathrm{n}}_{\mathrm{c},ij} = \frac{4}{3} E^* \left(R^*\right)^{\frac{1}{2}} \left(\alpha^{\mathrm{n}}\right)^{\frac{3}{2}} \boldsymbol{\delta}^{\mathrm{n}} \tag{2}$$

$$\boldsymbol{F}^{\mathrm{n}}_{\mathrm{d},ij} = -2\sqrt{\frac{5}{6}}\beta\sqrt{S^n m^*}\,\boldsymbol{v}^{n}_{rel} \tag{3}$$

$$\boldsymbol{F}^{\mathrm{t}}_{\mathrm{c},ij} = -\min\left\{8G^*\sqrt{R^*\alpha^{\mathrm{n}}}\,\alpha^{\mathrm{t}}, \mu_{\mathrm{s}}\left|\boldsymbol{F}^{\mathrm{n}}_{\mathrm{c},ij}\right|\right\}\boldsymbol{\delta}^{\mathrm{t}} \tag{4}$$

$$\boldsymbol{F}^{\mathrm{t}}_{\mathrm{d},ij} = -2\sqrt{\frac{5}{6}}\beta\sqrt{S^{\mathrm{t}} m^*}\,\boldsymbol{v}^{\mathrm{t}}_{\mathrm{rel}} \tag{5}$$

where E^* is the equivalent Young's modulus of the two colliding particles, R^* is the equivalent radius, α^{n} and α^{t} are the normal and tangential contact overlap, $\boldsymbol{\delta}^{\mathrm{n}}$ and $\boldsymbol{\delta}^{\mathrm{t}}$ are the normal and tangential unit vector, β is the damping ratio coefficient, S^{n} and S^{t} are the normal and tangential contact stiffness, m^* is the equivalent mass, $\boldsymbol{v}^{\mathrm{n}}_{\mathrm{rel}}$ and $\boldsymbol{v}^{\mathrm{t}}_{\mathrm{rel}}$ are normal and tangential components of the relative velocity, G^* is the equivalent shear modulus, μ_s is the static friction coefficient between particles.

The total torque $\boldsymbol{T}_{ij}$ caused by rolling friction is calculated by (6)

$$\boldsymbol{T}_{ij} = -\mu_{\mathrm{r}} \boldsymbol{F}^{\mathrm{n}}_{\mathrm{c},ij} \boldsymbol{r}_i \boldsymbol{\omega}_i \tag{6}$$

where μ_r is the rolling friction coefficient between particles, $\boldsymbol{r}_i$ is the vector directing from the center of particle i to the contact point, $\boldsymbol{\omega}_i$ is the vector of angular velocity.

III. Results And Discussion

Based on the above numerical calculation model, the evolution of flow patterns, residence times and average velocity distributions of particles in the heat exchanger are analyzed in this section. The dimensionless residence time (RT) [9] is defined by (7), which is adopted to evaluate the uniformity of the particle flow.

$$RT = \frac{t}{\bar{t}} \tag{7}$$

where t is the actual residence times, $\bar{t}$ is the mean residence time.

A. Evolution of flow patterns

Fig. 3 illustrates the snapshots obtained from the simulation at different times during the process of the particle flow, showing the evolution of flow patterns in the heat exchanger. At every beginning, all particles are motionless. Tracer layer is laid at the same level at the inlet of the heat exchanger. When the baffle starts moving, all particles move downward controlled by the baffle. As the tracer layer flows past the upper level of the tube bundle, form 0 s to 300 s, the particles which are right above the tube bundle originally are delayed gradually. From 1000 s to 1300 s, the tracer layer flows past the lower level of the tube bundle and reach the outlet while the particles right above the tube bundle originally are dragged and dispersed. The movement of particles which are near the walls falls behind gradually along the walls. The rest of particles almost keep the same level during the flow process.

B. Residence times of particles in the heat exchanger

As shown in Fig. 3, tracer layer is curved when it reached the outlet that indicates the residence times are different for particles in different positions. The residence times of the particles in the heat exchanger are shown in Fig. 4. The residence times of No. 2-5, which mean the residence times of particles that flow around tube bundle, are longer. The residence times of No. 1 and No. 6, which mean the residence times of particles that are the nearest to the walls, are also longer. The longest residence time, No. 5, is about 1.11. The residence times between No. 1 and No. 2 and between No. 5 and No. 6, which mean the residence times of particles that flow between the tube bundle and the walls, are generally shorter. The residence times between No. 3 and No. 4, which mean the residence times of particles that flow between two columns of the tube bundle, are the shortest on average. The shortest residence time is about 0.95.

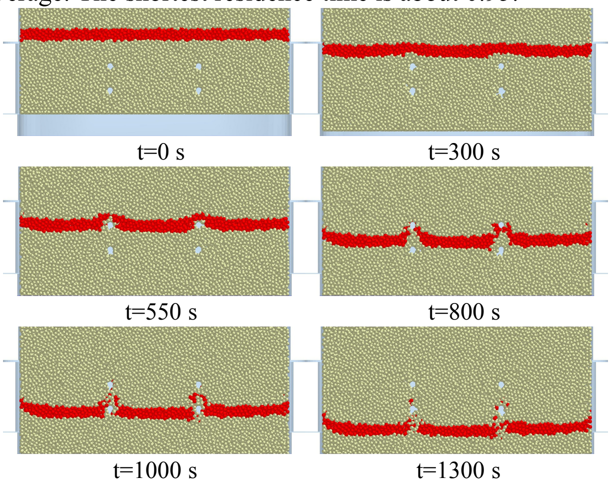

Fig. 3 Evolution of flow patterns in the heat exchanger

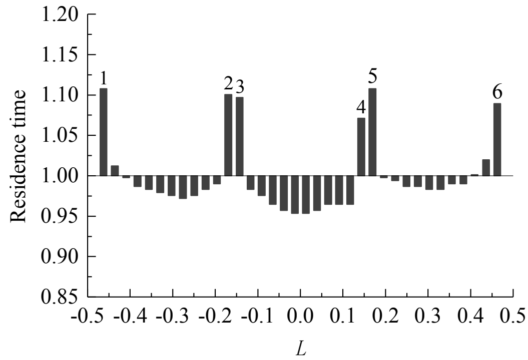

Fig. 4 Residence times of particles in the heat exchanger

Fig. 3 and Fig. 4 show that the effect of the geometry of the heat exchanger on the particle flow is significant. However, the longest residence time is about 1.11, and the shortest residence time is about 0.95 that indicates the slowest moving particles are about 10% slower than the average, and the fastest moving particles are less than 5% faster than the average. Therefore, the uniformity of the particle flow in the heat exchanger is good.

C. Average velocity distributions in the heat exchanger

As shown in Fig. 3 and Fig. 4, there are different flow regions in the heat exchanger. The flow region distributions in the heat exchanger are shown in Fig. 5. Flow around regions (FAR) where the particles flow around the tube bundle. Boundary layers (BL) which appear along the walls. The zone between two flow around regions is defined as major flow region of the center (MFRC). The zones between boundary layers and flow around regions are defined as major flow region of the left and the right (MFRL and MFRR).

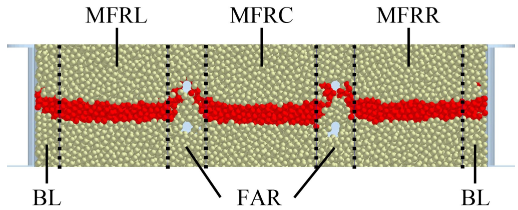

Fig. 5 Flow regions in the heat exchanger

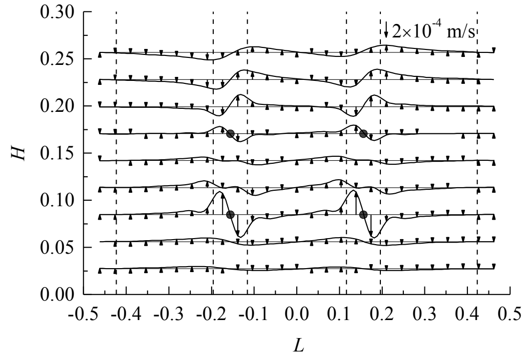

(a) Average horizontal velocity distributions

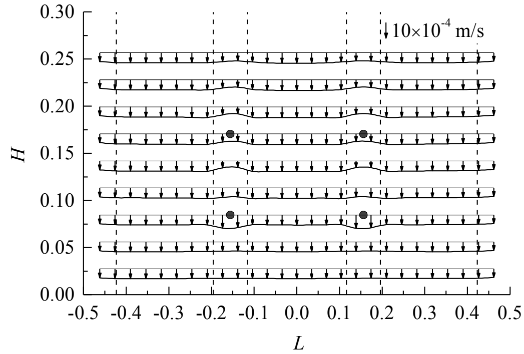

(b) Average vertical velocity distributions

Fig. 6 Average velocity distributions in heat exchanger

The average velocity distributions of particles in the heat exchanger are shown in Fig. 6. The dark gray circles represent the tube bundle. The length of the arrow indicates the velocity magnitude. Fig. 6(a) shows the average horizontal velocity distributions. The upward arrow indicates the direction of horizontal velocity is right, otherwise, the direction of horizontal velocity is left. Fig. 6(b) shows the average vertical velocity distributions, and the downward arrow means the direction of vertical velocity is downward. As shown in Fig. 6, the horizontal velocity and vertical velocity in the flow around regions change significantly. The horizontal velocity in the major flow regions and boundary layers is very small and can be ignored. The vertical velocity in the major flow regions and boundary layers has no significant changes.

As shown in Fig. 6(b), the average vertical velocity in the major flow region of the center is about 6.5×10^{-4} m/s, and the average vertical velocity in the major flow region of the left and the right is about 6.3×10^{-4} m/s. The movement of particles in the major flow regions is faster (Fig. 4). An explanation for this phenomenon is the reduction of the flow areas caused by the tube bundle which is placed into the heat exchanger. When the mass flow of particles is fixed, the velocity of particles will be increased absolutely. The ratio of the flow area in major flow region of the center to the flow area in major flow region of the left or the right is 0.97. Therefore, the average vertical velocity in the major flow region of the center is a bit larger than in the major flow region of the left and the right.

As shown in Fig. 6, the complex changes of the horizontal velocity and the vertical velocity in the flow around regions indicate that the effect of the tube bundle on the velocity of particles is significant. The average vertical velocity in the flow around regions, which is obviously smaller than in the major flow regions, is about 5.6×10^{-4} m/s. The trajectories of particles that are selected at the inlet are shown in Fig. 7. There are obvious phenomena of flow around for particles besides the tube bundle. The movement of particles which flow around the tube bundle is complex and delayed. Therefore, the movement of particles in the flow around regions is slower.

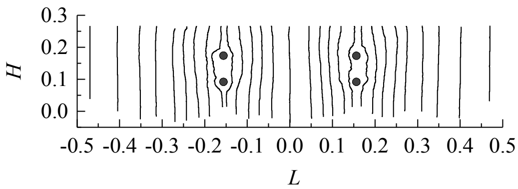

Fig. 7 Trajectories of particles in the heat exchanger

Furthermore, the direction of the horizontal velocity changes at the upper level of the tube bundle in the flow around regions, as shown in Fig. 6, which is caused by interaction between the particles and the tubes. First, the particles flow to both sides of the tube bundle and then flow back toward the tube bundle. This phenomenon, on the one hand, indicates that the flow around process can be divided into two stages of split-flow and back-flow, on the other hand, indicates that only the upper level of the tube bundle can split particles and the lower level of the tube bundle in the scope of back-flow.

As shown in Fig. 6, the largest horizontal velocity and vertical velocity appear below the lower level of the tube bundle in flow around regions, which is related to spaces without particles there. The spaces without particles below the tubes are shown in Fig. 8. The voidage is used to quantify the size of spaces without particles, as shown in Fig. 9. The voidages of area 1-4 in Fig. 8 are compared with the average voidage in major flow regions. The average voidage in area 3 and 4 is about 59.4%, which is much larger than the average voidage in area 1 and 2, 53.6%, and in major flow regions, 43.6%. In other words, the spaces without particles below the lower level of the tube bundle are much larger. When particles move there, the particles are less constrained and have larger spaces to accelerate. Therefore, the particles get the largest velocity below the lower level of the tube bundle.

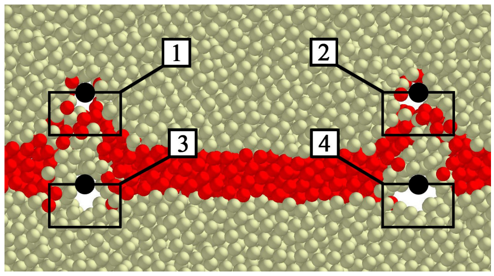

Fig. 8 Spaces without particles below tubes

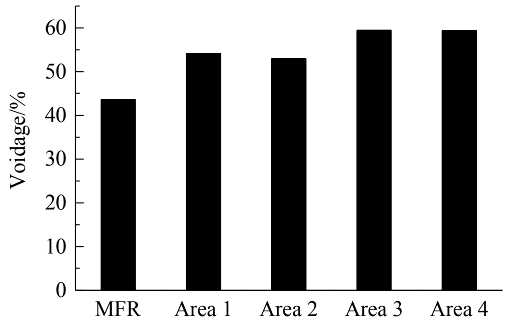

Fig. 9 Average voidages in major flow regions and parts

A boundary layer usually forms along a wall where the movement of particles would be slower than in major flow regions. The average vertical velocity in boundary layers is about 5.6×10^{-4} m/s, which is smaller than in major flow regions. When particle-wall friction is much greater than the particle-particle friction, a rupture zone appears near the wall, leading to the formation of the boundary layer [5].

IV. Conclusion

The effect of the particle flow on the heat transfer between the particles or between the particles and the heat exchanger is very important. The flow characteristics of particles in the heat exchanger are necessary to be studied to understand the behavior of the particle flow. In this paper, a discrete element model for the heat exchanger with immersed tubes was performed to analyze the behavior of the particle flow. The results show that although the effect of the immersed tubes on the particle flow is significant, the uniformity of the particle flow is good in the heat exchanger. Furthermore, there are different flow regions in the heat exchanger, including major flow region of the center, major flow regions of the left and the right, flow around regions and boundary layers. The research results of this paper provide useful references for the design and optimization of the heat exchanger.

References

[1] W. J. Yang, Z. Y. Zhou, A. B. Yu, "Particle scale studies of heat transfer in a moving bed" in *Powder Technology*, 2015, vol. 281, pp: 99-111.

[2] L. Kondic, "Simulations of two dimensional hopper flow" in *Granular Matter*, 2014, vol. 16, no. 2, pp: 235-242.

[3] Y. Yu, H. Saxén, "Discrete element method simulation of properties of a 3D conical hopper with mono-sized spheres" in *Advanced Powder Technology*, 2011, vol. 22, no. 3, pp: 324-331.

[4] Y. Zeng, F. G. Jia, Y. X. Zhang, X. Y. Meng, Y. L. Han, et al, "DEM study to determine the relationship between particle velocity fluctuations and contact force disappearance" in *Powder Technology*, 2017, vol. 313, pp: 112-121.

[5] C. González-Montellano, Á. Ramírez, E. Gallego, F. Ayuga, "Validation and experimental calibration of 3D discrete element

models for the simulation of the discharge flow in silos" in *Chemical Engineering Science*, 2011, vol. 66, no. 21, pp: 5116-5126.
[6] G. H. Rong, S. C. Negi, J. C. Jofriet, "Simulation of Flow Behaviour of Bulk Solids in Bins. Part 2: Shear Bands, Flow Corrective Inserts and Velocity Profiles" in *Journal of Agricultural Engineering Research*, 1995, vol. 62, no. 4, pp: 257-269.
[7] J. T. Wu, B. B. Jiang, J. Z. Chen, Y. R. Yang, "Multi-scale study of particle flow in silos" in *Advanced Powder Technology*, 2009, vol. 20, no. 1, pp: 62-73.
[8] S. C. Yang, S. S. Hsiau, "The simulation and experimental study of granular materials discharged from a silo with the placement of inserts" in *Powder Technology*, 2001, vol. 120, no. 3, pp: 244-255.
[9] K. L. Iroba, J. Mellmann, F. Weigler, T. Metzger, E. Tsotsas, "Particle velocity profiles and residence time distribution in mixed-flow grain dryers" in *Granular Matter*, 2011, vol. 13, no. 2, pp: 159-168.

Daichang Guo is working towards the M.S. degree in the School of Transportation and Vehicle Engineering, Shandong University of Technology, Zibo, Shandong Province, China. His main research field is heat and mass transfer and technologies for efficient utilization of waste heat.

Bin Zheng works as an associate professor in the School of Transportation and Vehicle Engineering, Shandong University of Technology. He is specialized in recovery and utilization of waste heat from solid materials and utilization of energy from low quality gas. He is the corresponding author of this paper.

Haotian Liang is working towards the M.S. degree in the School of Transportation and Vehicle Engineering, Shandong University of Technology, Zibo, Shandong Province, China. His main research field is heat and mass transfer and technologies for efficient utilization of waste heat.

Yongqi Liu works as a professor in the School of Transportation and Vehicle Engineering, Shandong University of Technology. He is a Ph. D. supervisor in Shandong University of Technology and Shandong University. He is devoted to the technologies for utilization of energy from low quality gas and saving energy, and technologies for efficient combustion and utilization of waste heat. He has authored or coauthored more than 100 publications in international journals.

Peng Sun graduated from Ph. D. and works as a lecturer in the School of Transportation and Vehicle Engineering, Shandong University of Technology. His main research field is utilization of waste heat and heat transfer and combustion of gas-solid flow.